

Plasmapause undulation of 17 April 2002

J. Goldstein,¹ B. R. Sandel,² M. R. Hairston,³ and S. B. Mende⁴

Received 11 March 2004; revised 1 July 2004; accepted 13 July 2004; published 10 August 2004.

[1] We report IMAGE EUV observations of a striking undulatory motion of the plasmapause that occurred on 17 April 2002, in which a large ripple propagated westward across the duskside plasmapause. From the plasmapause motion we infer a peak E-field of ≈ 3 mV/m associated with the undulation, and estimate the undulation's equatorial azimuthal speed to be 0.9 rad/hr $\approx 4 R_E$ /hr, corresponding to ≈ 1 km/s in the ionosphere (using an $R^{3/2}$ dependence to map from the equator). Because DMSP ion drift data at 850 km altitude show the presence of a subauroral polarization stream (SAPS) flow channel ≈ 1 km/s at the same location and time as the undulation, we assert that SAPS was responsible for removal of plasma during the undulation. The SAPS apparently formed in response to a 19:00 UT substorm onset. **INDEX TERMS:** 2712 Magnetospheric Physics: Electric fields (2411); 2768 Magnetospheric Physics: Plasmasphere; 2788 Magnetospheric Physics: Storms and substorms. **Citation:** Goldstein, J., B. R. Sandel, M. R. Hairston, and S. B. Mende (2004), Plasmapause undulation of 17 April 2002, *Geophys. Res. Lett.*, 31, L15801, doi:10.1029/2004GL019959.

1. Introduction

[2] Since 2000 the IMAGE extreme ultraviolet (EUV) imager has routinely obtained global images of the plasmasphere [Sandel et al., 2003]. EUV detects 30.4-nm sunlight resonantly scattered by plasmaspheric He⁺ ions, producing images that capture the portion of the plasmasphere corresponding to electron densities above ≈ 40 cm⁻³ [Goldstein et al., 2003c; Moldwin et al., 2003]. Analysis of an EUV image often involves identifying a steep gradient in the He⁺ distribution, and mapping its location to the equatorial plane [Roelof and Skinner, 2000], yielding global plasmapause curves that agree with in situ measurements to within a fraction of an Earth radius (R_E) [Spasojević et al., 2003; Moldwin et al., 2003].

[3] Because the plasmasphere is composed of cold (≈ 1 eV) plasma subject primarily to $E \times B$ drift, the location and shape of the plasmapause is a useful diagnostic of the inner magnetospheric convection field. It is well established that dayside magnetopause reconnection (DMR) during southward interplanetary magnetic field (IMF) imposes a dawn-dusk E-field that drives sunward convec-

tion in the inner magnetosphere. Consistent with this, sunward motions of the plasmapause in EUV images have been strongly correlated with intervals of southward IMF [Goldstein et al., 2003a; Spasojević et al., 2003; Goldstein et al., 2003b]. There is also good evidence that auroral substorm dipolarizations provide a strong sunward push to the plasmaspheric plasma [e.g., Carpenter and Smith, 2001, and references therein]. In global EUV images, such substorm-driven plasmapause motion has not yet been directly or conclusively observed, although Goldstein et al. [2003a] argued that substorm E-fields probably contributed to an EUV-observed erosion event on 10 July 2000.

[4] During auroral activity, feedback between the ring current (i.e., innermost plasmasheet) and the ionosphere creates the subauroral polarization stream (SAPS) [Foster and Burke, 2002; Anderson et al., 2001; Burke et al., 1998]. Spatial separation between the inner edges of the ion and electron plasma sheets produces field-aligned currents (FAC) at the two edges that are completed by a poleward-flowing Pedersen current in the nightside subauroral ionosphere. The flow of this current through the low conductivity subauroral ionosphere produces strong poleward E-fields (which in turn can further reduce the ionospheric conductivity [Anderson et al., 2001]). Thus, ionospheric SAPS are strong poleward E-fields found (on average) 3–5 degrees magnetic latitude (Λ) below the auroral oval, concentrated most strongly in the dusk/pre-midnight sector [Foster and Vo, 2002]. In the equatorial plane this maps to a radially-narrow (1–2 R_E) channel of westward flows (i.e., radial E-fields) that affects the plasmasphere by intensifying duskside convection [Goldstein et al., 2003b].

[5] In this letter we report EUV observations from 17 April 2002 of a striking undulatory motion of the plasmapause consisting of the formation and removal of a duskside plasmapause bulge. We will provide observational evidence that a SAPS flow channel removed the bulge plasma, and speculate that a 19:00 UT substorm onset caused the global sunward convection enhancement responsible for the entire event.

2. Plasmapause Undulation

2.1. Plasmapause Motion

[6] Figure 1 shows IMAGE EUV observations from 19:05–20:37 UT on 17 April 2002. The top row contains EUV images, mapped to the magnetic equator. The color/intensity is proportional to line-of-sight-integrated He⁺ column abundance, in arbitrary units. The plasmasphere is the green/white haze surrounding the Earth (drawn in the center). Each plot in the bottom row of Figure 1 shows the manually-extracted plasmapause from the EUV image directly above it. The image quality in Figures 1a–1d suffers from two problems. First, the images contain above-normal background noise (dark green speckling

¹Space Science and Engineering Division, Southwest Research Institute, San Antonio, Texas, USA.

²Lunar and Planetary Laboratory, University of Arizona, Tucson, Arizona, USA.

³Center for Space Sciences, University of Texas at Dallas, Richardson, Texas, USA.

⁴Space Sciences Laboratory, University of California, Berkeley, California, USA.

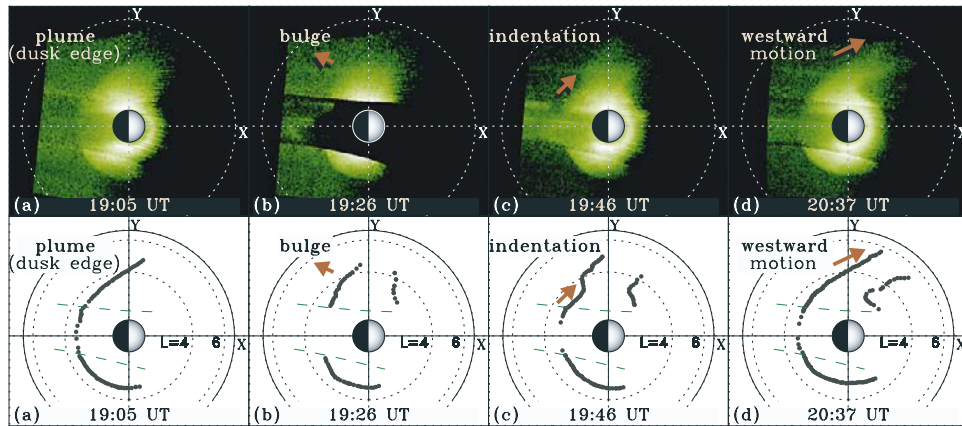


Figure 1. Four snapshots of the 17 April 2002 undulation, in which a duskside plasmopause bulge formed and was subsequently stripped away by a westward-propagating indentation. Upper: IMAGE EUV equatorial He^+ abundance. Saturated counts in the center camera (dashed lines, lower panel) and partial loss of dayside signal are both artifacts of sunlight contamination. Lower: Manually extracted plasmopause. Solid lines: X and Y axes (SM coordinates) and geosynchronous orbit. Dotted lines: $L = 4, 6$.

outside the plasmopause), probably due to the very disturbed geomagnetic conditions (see below). Second, due to the viewing geometry the images contain significant sunlight contamination, causing signal attenuation on the dayside, saturation or turning off of the center camera, and some streaking in the top 1/3 of the image. For reference, the center camera edges are indicated by the dashed lines in the bottom panels. Gaps in the extracted plasmapauses (lower panels) are where sunlight contamination prevented plasmopause identification. Manual plasmopause extraction involves some subjective uncertainty which we estimate (based on the work of Goldstein *et al.* [2003c]) to be $\approx 0.1L$ on the nightside where the plasmopause gradient is steep, and $\leq 0.4L$ near dusk.

[7] 17 April 2002 was the first day of a large geomagnetic storm; at 18 UT, $\text{Dst} \approx -98$ nT and $\text{Kp} > 6$. (For more about the 17 April storm, see Liemohn *et al.* [2004].) Typical of these geomagnetic conditions, the plasmasphere in the 19:05 UT EUV image (Figure 1a) shows evidence of a prior period of erosion; the nightside plasmopause has both a sharp radial gradient and a smooth MLT-shape that is roughly circular (at $L \approx 3.3$) east of 2000 MLT and contains evidence of a drainage plume near dusk.

[8] Figures 1a–1d summarize the plasmopause undulation event. The strongest and most conspicuous motion was a ripple (i.e., azimuthal gradient in the plasmopause radius) that formed and propagated westward along the duskside plasmopause. At 19:26 UT (Figure 1b) the ripple was shallow, consisting of a mild $0.4 R_E$ bulge west of 2000 MLT, and a mild $0.4 R_E$ indentation east of 2000 MLT. After 19:36 UT the eastern edge of the ripple was steepened by a westward-propagating $1 R_E$ indentation that apparently stripped away the mild bulge. At 19:46 UT (Figure 1c) this indentation/ripple was located at 2000–2100 MLT. The formation and removal of the bulge produced a dramatic global undulatory motion of the duskside plasmopause that has been neither identified nor explicitly predicted in previous studies. Unlike typical erosion events seen by EUV [Goldstein *et al.*, 2003a] in which the plasmopause moved $\geq 2 R_E$ inward, the net inward displacement for the 17 April undulation was small;

after the undulatory motion ended (20:37 UT, Figure 1d) the duskside plasmopause returned to its approximate original location (19:05 UT, Figure 1a).

2.2. Plasmopause Electric Field

[9] We used the technique of Goldstein *et al.* [2004] to infer for this event the electric field E_π , defined as the component of E-field tangent to the moving plasmopause. (Note E_π has contributions from both radial and azimuthal E-fields.) Figure 2a plots E_π vs. UT (vertical axis) and MLT (horizontal axis) between 18:04–21:28 UT on 17 April 2002. The times of the four snapshots in Figures 1a–1d are indicated by the four broken horizontal lines labeled a–d. E_π intensity (in mV/m) is given by the colorbar. Crude error-propagation analysis yields 0.1–0.2 mV/m uncertainty in E_π due to subjectivity in the manually-extracted plasmopause alone. Line plots of E_π vs. UT contain noise-like fluctuations of amplitude 0.4–0.5 mV/m, which we take as an estimate of the total uncertainty in E_π .

[10] For inward motion of the plasmopause, $E_\pi < 0$ (green, yellow, orange, or red); for outward motion, $E_\pi > 0$ (dark blue). Figure 2a shows that the 17 April 2002 event began at 19:05 UT (horizontal line ‘a’) with an indentation

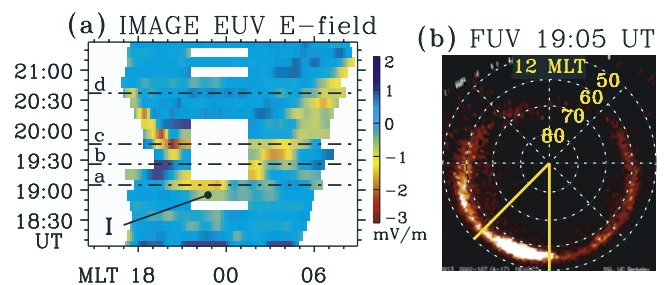


Figure 2. (a) Electric field E_π tangent to the moving plasmopause vs. UT and MLT. Colorbar gives strength in mV/m (white = no data). (b) IMAGE FUV SII3 electron aurora at 19:05 UT, vs. magnetic latitude (Λ) and local time (noon MLT at top). Substorm onset occurred 2100–2400 MLT (yellow lines).

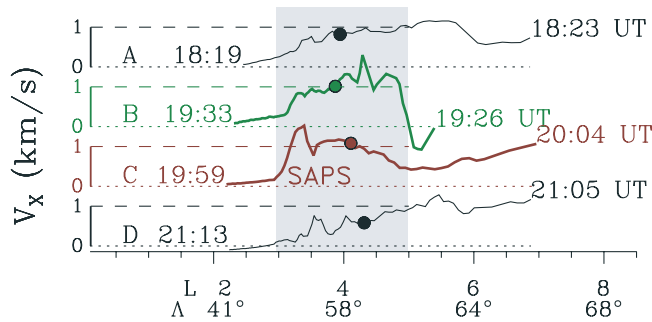


Figure 3. The 17 April DMSP F13 drift meter data (850 km altitude): sunward flow speed (km/s) vs. dipole L and Λ for 4 successive passes through duskside subauroral region. MLT of four intervals: (A) 1816–1818, (B) 1805–1808, (C) 1823–1831, (D) 1823–1901. SAPS (trace C) flows are evident at the same time and location as the plasmopause undulation.

(‘I’) of the 2100–2400 MLT plasmopause with associated westward $E_{\pi} \approx -1.2$ to -1.5 mV/m. After 19:05 UT, an effect propagated along the plasmopause both eastward and westward from this pre-midnight sector, producing the V-shaped signature in Figure 2a. (The vertex of the ‘V’ is at ‘I’.) The westward-moving effect (the left half of the ‘V’) is the manifestation in E_{π} of the duskside undulation (Figure 1). Outward bulging of the post-dusk plasmopause (see Figure 1b) shows up as blue pixels ($E_{\pi} \approx 1.3$ mV/m) between 1900–2100 MLT during 19:16–19:26 UT. The approximately linear red/yellow ($E_{\pi} \approx -2$ to -3 mV/m) signature from (2100 MLT, 19:40 UT) to (1730 MLT, 20:40 UT) is the westward-moving indentation that stripped off the outer edge of the plasmopause. From this linear signature we estimate the azimuthal speed of the undulation to be ≈ -3.5 MLT/UT. The eastward-moving branch, from (0200 MLT, 19:20 UT) to (0800 MLT, 21 UT), is the signature of a subtler undulatory plasmopause motion, with a smaller plasmopause displacement (ripple) that propagated from ‘I’ to the dawnside at an azimuthal speed ≈ 3.6 MLT/UT. This eastward-propagating ripple is not an artifact of our analysis to infer E_{π} . The azimuthal flow speed at both dawn and dusk was $|\dot{\phi}| \approx 0.9$ rad/hr, or $V_{\phi} \approx 4 R_E/\text{hr}$ at $L = 4$. The peak E_{π} intensity near dusk (≈ 3 mV/m, dark red color) was about 1.7 times that of dawn (≈ 1.8 , orange).

2.3. Substorm-Driven Convection

[11] From Figure 2a we see that the duskside undulation was part of a larger convection effect with a clear ripple signature on the plasmopause that propagated sunward from pre-midnight MLT. It is likely that this convection effect was primarily driven by a substorm onset (with associated dipolarization of the magnetotail). The SI13 camera of the IMAGE far ultraviolet (FUV) imager obtains global pictures of the electron aurora in 135.6-nm light [Mende *et al.*, 2000]. Figure 2b is a polar-projected auroral image from 19:05 UT, vs. magnetic latitude (Λ) and MLT. This FUV snapshot shows a substorm onset signature below $60^{\circ}\Lambda$ and between 2100–2400 MLT, i.e., inside the wedge-shaped region bounded by the two thick yellow lines. The first evidence of this onset feature occurred at 19:00 UT (not shown). Recalling Figure 2a, it is remarkable that the onset

feature occurred in the same MLT range, and at roughly the same time, as the first plasmopause indentation (‘I’) seen by EUV at 19:05 UT. This is strong circumstantial evidence that the substorm onset caused the convection enhancement responsible for the entire event, in which case this study contains the first global observations of the direct effects on the plasmopause of substorm-dipolarization-driven convection.

[12] We now discuss the possible role of dayside magnetopause reconnection (DMR) driven convection in the initiation of enhanced convection at 19:05 UT. From measurements of the interplanetary magnetic field (IMF) made by the ACE spacecraft [Stone *et al.*, 1998] (not shown), the IMF polarity at the dayside magnetopause changed to a strongly southward (-20 nT) orientation at about 18:30 UT. About 35 minutes later the initial plasmopause indentation occurred; this time delay is consistent with 20–30-minute magnetopause-to-plasmasphere delays observed by Goldstein *et al.* [2003a]. However, we speculate that DMR-driven convection played a minor role. The undulation occurred after 10 hours of stormtime enhanced convection, so that further increases in DMR-driven convection would have a minimal effect on the already eroded plasmasphere. As noted earlier, the net inward plasmopause displacement caused by the convection enhancement was small, inconsistent with typical DMR-driven nightside erosion, but perhaps consistent with the passage of a transient convective impulse that one might expect during a substorm dipolarization.

2.4. Sub-Auroral Polarization Stream

[13] The EUV observations of Figure 1 suggest qualitatively that the removal of the duskside bulge during the undulation was caused by a westward-moving flow such as a SAPS flow channel. In this section we present evidence of SAPS at the time and place of the undulation.

[14] Figure 3 displays ion drift meter data obtained during 4 successive passes (‘A’–‘D’) of the Defense Meteorological Satellite Program (DMSP) F13 spacecraft [Greenspan *et al.*, 1986] through the duskside subauroral ionosphere (≈ 850 km altitude). Sunward flow speed V_x (km/s) is plotted vs. dipole L and magnetic latitude Λ along the DMSP F13 orbit. (Note: the ‘sunward’ flow is actually the inertial-frame velocity component perpendicular to the \sim dawn-dusk F13 trajectory.) Each pass is labeled by start and stop UT (e.g., pass A was obtained between 18:20–18:23 UT), and the equatorward edge of the electron aurora (determined from DMSP particle data, not shown) is given by the filled circle.

[15] The flow profile of pass C (19:59–20:04 UT) contains a broad peak ($V_x > 1$ km/s), roughly $2L$ wide with a narrow ‘spike’ at the inner edge. This profile is typical of SAPS, although the broad peak does extend slightly above the auroral edge (the red circle). The four DMSP passes depict the birth and death of this SAPS feature, which apparently began to form after about 19:30 UT (later half of pass B), was fully-formed in pass C, and gone by 21:00 UT (pass D). The interval of SAPS activity (within 19:30–21:00 UT) is consistent with that of the undulation (19:36–20:37 UT). The L -range of enhanced flows also agrees with that of the undulation ($L = 3$ – 5 , the gray shaded region in Figure 3). Earlier we inferred an azimuthal flow speed of

$4 R_E/\text{hr}$ for the undulation. Mapping to 850 km using an $R^{3/2}$ velocity dependence (good for dipole B-field) yields ionospheric flow speed ≈ 1 km/s, in good agreement with the observed SAPS magnitude. Thus, duskside SAPS were seen by DMSP at the same time and place, and with the same intensity, as the flows associated with the removal of the duskside bulge during the undulation. We therefore assert that SAPS was responsible for removing the mild bulge that had formed before 19:36 UT.

[16] Enhanced sunward convection injects ring current plasma into the inner magnetosphere, producing pressure gradients that drive field-aligned currents (FAC) into the ionosphere to produce the SAPS [Anderson et al., 2001; Burke et al., 1998; Foster and Burke, 2002]. In this 17 April 2002 event, the primary source of the SAPS ring current ions seems to have been sunward convection resulting from the 19:00 UT substorm dipolarization that caused the initial plasmopause indentation ('I' in Figure 2a). But what caused the mild duskside bulge (Figure 1b) to form just prior to the SAPS? One possibility is that plasmaspheric plasma was removed from pre-midnight MLT and convected westward (i.e., sunward), and this redistribution of plasma created a mild bulge. A second possibility is that the enhanced post-dusk ring current pressure (from the injection) produced a local mild antisunward stretching of the geomagnetic field lines, and that cold, $E \times B$ -drifting plasmaspheric plasma was thus pulled outward (R. W. Spiro, personal communication, 2004).

3. Conclusions

[17] In this letter we have reported IMAGE EUV observations of the duskside undulation of 17 April 2002, the first identification of this type of plasmopause motion. We used EUV-inferred electric field analysis to gain quantitative understanding of the dynamics and timing of this event. From its signature in E_π we estimated the undulatory ripple's azimuthal speed to be $4 R_E/\text{hr}$ (or 1 km/s in the ionosphere).

[18] We demonstrated that the 19:36–20:37 UT undulation was due to the presence of a SAPS flow channel observed by DMSP in the same range of MLT, L and UT as the undulation. The observed SAPS flows (1 km/s) are consistent with the EUV-observed undulation speed. The SAPS formed in response to a pre-midnight convection enhancement whose main cause was most likely a substorm onset. Thus, the 17 April EUV images contain the first global observations of some of the details of how both SAPS and substorm dipolarization affect the plasmasphere. A more comprehensive study of the interplay of the 17 April substorm, ring current, SAPS and plasmasphere will be reported in a future paper.

[19] **Acknowledgments.** Access to ACE data was provided by N. Ness, C. Smith, D. McComas and the ACE science center. We thank both reviewers of this paper for their exceptionally helpful and expert

comments, which greatly improved the paper. We are grateful for the following support: NASA SEC-GI NAG5-12787 (J. G.); NASA NAS5-96020 (B. R. S., S. B. M.); NAG5-9297 (M. R. H.).

References

- Anderson, P. C., D. L. Carpenter, K. Tsuruda, T. Mukai, and F. J. Rich (2001), Multisatellite observations of rapid subauroral ion drifts (SAID), *J. Geophys. Res.*, *106*, 29,585.
- Burke, W. J., et al. (1998), Electrodynamics of the inner magnetosphere observed by CRRES and DMSP during the magnetic storm of June 4–6, 1991, *J. Geophys. Res.*, *103*, 29,399.
- Carpenter, D. L., and A. J. Smith (2001), The study of bulk plasma motions and associated electric fields in the plasmasphere by means of whistler-mode signals, *J. Atmos. Solar Terr. Phys.*, *63*, 1117.
- Foster, J. C., and W. J. Burke (2002), SAPS: A new categorization for subauroral electric fields, *Eos Trans. AGU*, *83*, 393.
- Foster, J. C., and H. B. Vo (2002), Average characteristics and activity dependence of the subauroral polarization stream, *J. Geophys. Res.*, *107*(A12), 1475, doi:10.1029/2002JA009409.
- Goldstein, J., B. R. Sandel, W. T. Forrester, and P. H. Reiff (2003a), IMF-driven plasmasphere erosion of 10 July 2000, *Geophys. Res. Lett.*, *30*(3), 1146, doi:10.1029/2002GL016478.
- Goldstein, J., B. R. Sandel, P. H. Reiff, and M. R. Hairston (2003b), Control of plasmaspheric dynamics by both convection and sub-auroral polarization stream, *Geophys. Res. Lett.*, *30*(24), 2243, doi:10.1029/2003GL018390.
- Goldstein, J., M. Spasojević, P. H. Reiff, B. R. Sandel, W. T. Forrester, D. L. Gallagher, and B. W. Reinisch (2003c), Identifying the plasmopause in IMAGE EUV data using IMAGE RPI in situ steep density gradients, *J. Geophys. Res.*, *108*(A4), 1147, doi:10.1029/2002JA009475.
- Goldstein, J., R. A. Wolf, B. R. Sandel, and P. H. Reiff (2004), Electric fields deduced from plasmopause motion in IMAGE EUV images, *Geophys. Res. Lett.*, *31*, L01801, doi:10.1029/2003GL018797.
- Greenspan, M. E., P. B. Anderson, and J. M. Pelagatti (1986), Characteristics of the thermal plasma monitor (SSIES) for the Defense Meteorological Satellite Program (DMSP) spacecraft S8 through S10, *Tech. Rep. AFGL-TR-86-0227*, Air Force Geophys. Lab., Hanscom AFB, Mass.
- Liemohn, M. W., A. J. Ridley, D. L. Gallagher, D. M. Ober, and J. U. Kozyra (2004), Dependence of plasmaspheric morphology on the electric field description during the recovery phase of the 17 April 2002 magnetic storm, *J. Geophys. Res.*, *109*, A03209, doi:10.1029/2003JA010304.
- Mende, S. B., et al. (2000), Far ultraviolet imaging from the IMAGE spacecraft: 3. Spectral imaging of Lyman- α and OI 135.6 nm, *Space Sci. Rev.*, *91*, 287.
- Moldwin, M. B., B. R. Sandel, M. Thomsen, and R. Elphic (2003), Quantifying global plasmaspheric images with in situ observations, *Space Sci. Rev.*, *109*, 47.
- Roelof, E. C., and A. J. Skinner (2000), Extraction of ion distributions from magnetospheric ENA and EUV images, *Space Sci. Rev.*, *91*, 437.
- Sandel, B. R., J. Goldstein, D. L. Gallagher, and M. Spasojević (2003), Extreme ultraviolet imager observations of the structure and dynamics of the plasmasphere, *Space Sci. Rev.*, *109*, 25.
- Spasojević, M., J. Goldstein, D. L. Carpenter, U. S. Inan, B. R. Sandel, M. B. Moldwin, and B. W. Reinisch (2003), Global response of the plasmasphere to a geomagnetic disturbance, *J. Geophys. Res.*, *108*(A9), 1340, doi:10.1029/2003JA009987.
- Stone, E. C., A. M. Frandsen, R. A. Mewaldt, E. R. Christian, D. Margolies, J. F. Ormes, and F. Snow (1998), The Advanced Composition Explorer, *Space Sci. Rev.*, *86*, 1.

J. Goldstein, Space Science and Engineering Division, Southwest Research Institute, 6220 Culebra Road, San Antonio, TX 78228, USA. (jgoldstein@swri.edu)

M. R. Hairston, Center for Space Sciences, University of Texas at Dallas, P.O. Box 830688 FO22, Richardson, TX 75083, USA.

S. B. Mende, Space Sciences Laboratory, University of California, Berkeley, 7 Gauss Way, Berkeley, CA 94720, USA.

B. R. Sandel, Lunar and Planetary Laboratory, University of Arizona, Tucson, AZ 85721, USA.